

Improving the hot corrosion resistance of γ/γ' in Fe-Ni superalloy coated with Cr_3C_2 -20NiCr and NiCrAlY using HVOF thermal spray coating

Selly Septianissa^{1,*}, Budi Prawara², Eddy Agus Basuki¹, Erie Martides², Edy Riyanto^{2,*}

¹ Department of Metallurgical Engineering, Faculty of Mining and Petroleum Engineering, Institut Teknologi Bandung, Bandung 40132, Indonesia

² Research Center for Advanced Material, National Research and Innovation Agency, Serpong 15314, Indonesia

*E-mail: edy.riyanto@brin.go.id; selly.septianissa@yahoo.co.id

Received: 31 July 2022 / Accepted: 4 September 2022 / Published: 30 November 2022

In this study, the corrosion resistance of uncoated and coated Ferro Nickel-based superalloy (Fe-Ni) strengthened by the precipitation of the ordered fcc γ' $\text{Ni}_3(\text{Al}, \text{Ti})$ was evaluated by cyclic hot corrosion testing. Fe-Ni was coated with Cr_3C_2 -20NiCr and NiCrAlY by high-velocity oxy-fuel thermal spray coating and then tested with a mixture solution of 75 wt.% Na_2SO_4 + 25 wt.% NaCl at 900 °C for 50 cycles. Scanning electron microscopy combined with energy dispersive spectroscopy and X-ray diffraction were performed to investigate the corrosion products and mechanisms. The kinetics of corrosion was evaluated by measuring the mass changes. The experimental results show that the uncoated superalloy with precipitation strengthened in the substrate suffered by spallation and sputtering of the oxide scale. The presence of Cr_3C_2 -20NiCr and NiCrAlY coating layers could significantly improve the hot corrosion resistance with the NiCrAlY layer showing a better protection performance than Cr_3C_2 -20NiCr. A precipitation-strengthened Fe-Ni superalloy with NiCrAlY coating reduced the overall weight gain, which could be attributed to the formation of protective oxide of chromium, nickel, aluminum, and their spinel. The lower corrosion performance of the superalloy coated with Cr_3C_2 -20 NiCr layer was due to the presence of chlorine element, which increased the corrosion attack through chlorination.

Keywords: Hot corrosion, thermal spray coating, superalloys, NiCrAlY coating, Cr_3C_2 -20 NiCr coating.

1. INTRODUCTION

Many power plant components are made of Fe-Ni-based superalloys due to their high resistance to oxidation, wear, and creep and good thermomechanical properties at high temperatures. The Fe-Ni superalloy used in this study is similar to the A286 alloy, which is widely used in the gas turbine industry

due to its high strength and excellent corrosion resistance at intermediate temperatures [1-2]. This alloy is strengthened by the precipitation of the ordered fcc γ' Ni₃(Al, Ti) [2-4], which mostly referred to the acid environments such as sulfuric acid, chlorine, and good hydrogen service environment [5-6]. The presence of these elements in the alloy contributes to its excellent hot corrosion resistance than semi-austenitic precipitation hardened stainless steels, which can be attributed to the structural hardening by precipitation of the ordered γ' phase [2,7].

Degradation due to hot corrosion is the main failure in high-temperature environments of boilers, gas turbines, power plant superheaters, industrial waste incinerators, metallurgical furnaces, and marine engines. This is caused by the thin deposits of molten salts, especially alkali metal sulfates, chlorides, and salt mixtures (e.g., Na₂SO₄, NaCl, V₂O₅, NaVO). The impurities absorbed from the atmosphere or fuel react to form Na₂SO₄, whereas NaCl enters the system with intake air. Na₂SO₄ is obtained when NaCl in the air reacts with SO₃ (i.e., partially oxidized from SO₂ during the combustion of fuel) and water vapor at the combustion temperature [8-11]. The presence of NaCl in the molten salts creates a more aggressive environment compared with pure Na₂SO₄, which only provides corrosion protection when Al₂O₃ is formed, and Cr₂O₃ is not able to protect the substrate against the hot corrosion induced by chlorine [12-15].

Coatings can add value to products by providing corrosion resistance of the substrate material to improve the life of the components. Overlay coating performed better in aggressive environments from hot corrosion that can be deposited by thermal spray technologies like high-velocity oxy-fuel (HVOF), cold spray, plasma spray, electron beam physical vapor deposition, arc spray, and detonation gun [16-18]. HVOF spray is a cost-effective thermal spray system that provides a hard, less porous, and dense coating that can adhere to the substrate [19-24]. To protect certain components in harsh conditions, some thermal spray materials such as NiCr, Cr₃C₂, and NiCrAlY have been utilized to improve the performance in hot environment [25-29]. In this study, the presence of films created by HVOF thermal spray coating could greatly improve the corrosion resistance of Fe-Ni superalloys in hot environments, with NiCrAlY coating material providing higher corrosion protection than the Cr₃C₂-NiCr layer.

2. EXPERIMENTAL DETAILS

Ferro Nickel-based superalloy was used as a substrate. The chemical composition of the superalloy is shown in Table 1. The alloys were casted by using a direct current electric arc furnace to produce the desired γ' -Ni₃Al in 45 min. Then, a homogenization process on horizontal furnaces was conducted in an inert environment. The homogenization process in the experiment was carried out at 1150 °C for 5 h. All samples were subjected to solution treatment at 980 °C for 1 h followed by water quenching. Then, the samples were isothermally aged at 840 °C for 4 h to obtain the desired microstructure.

Table 1. Chemical composition (wt.%) of Fe-Ni based superalloy

Alloy	Fe	Ni	Al	Cr	Ti	Mo
Fe-Ni alloy	balance	26	0.8	15	2	0.25

The specimens were cut to 15 mm × 15 mm × 3 mm by using a wire cutter. All surfaces were ground with 60, 100, 120, 1000, 1200, 1500, 2000, and 5000 grid SiC papers and then cleaned with acetone to remove the oxide scale. The specimen weight was measured by using a precision balance with an accuracy of 10⁻⁴ g. Furthermore, samples were grit blasted with alumina paste to increase the surface roughness, which improved the adhesion. To ensure the cleanliness of the substrate surfaces, the sample was rinsed using distilled water and acetone. The Cr₃C₂-20%NiCr and NiCrAlY powder were deposited onto the superalloy material by using HVOF thermal spray coating. The parameter used for the thermal spraying process is shown in Table 2.

Table 2. Parameter for the HVOF thermal spraying process

Parameters	Values
Oxygen pressure	8 bar
Oxygen flow rate	270 L/min
Propane pressure	5.5 bar
Propane flow rate	62.4 L/min
Nitrogen pressure	5 bar
Nitrogen flow rate	8 L/min
Air pressure	6.2 bar
Spray distance	250 mm

Cyclic hot corrosion evaluation was performed on the uncoated Fe-Ni superalloy and superalloy coated with Cr₃C₂-20%NiCr and NiCrAlY layers by using molten salt of 75 wt.% Na₂SO₄ + 25 wt.% NaCl for 13 cycles. Each cycle consisted of 1 h heating at 900 °C in the muffle furnace followed by 20 min cooling at room temperature. The specimens were heated up to ~230 °C (30 min) in the oven to achieve good adherence of the salt layer. The salt solution was applied on the warm polished specimen (3–5 mg/cm²) by using a brush. The salt-coated specimens were dried at 110 °C for 2 h. After drying, the sample weight was measured again. The samples were placed in a porcelain crucible during the weight measurement. Thereafter, the porcelain crucible with samples was placed inside the furnace for 1 h at 900 °C. During the hot corrosion testing process, the weight of the crucible containing the sample along with the spalled material fallen, was included in weight measurement at the end of each cycle to ensure the corrosion kinetics. After completing the hot corrosion tests, the phase was identified by X-ray diffraction (XRD, RIGAKU Smartlab 3kW 2080B212 type) and the result was conformed with match application. The cross sections, surface morphology, and compositions of corrosion products were investigated by scanning electron microscopy (SEM)/energy dispersive spectroscopy (EDS) (SU3500, Hitachi High-Tech America).

3. RESULTS AND DISCUSSION

Fig. 1 shows the cross-sectional optical images of Fe-Ni superalloy coated with $\text{Cr}_3\text{C}_2\text{-NiCr}$ and NiCrAlY by HVOF thermal spray coating (Figs. 1(a)–(b)). As shown in the figure, $\text{Cr}_3\text{C}_2\text{-NiCr}$ and NiCrAlY materials could be successfully deposited onto the Fe-Ni superalloy by HVOF thermal spray coating. The $\text{Cr}_3\text{C}_2\text{-NiCr}$ and NiCrAlY layers were uniform and adhered to the substrate material with thicknesses of approximately 63.72 and 72.04 μm , respectively. However, some micropores emerged in the deposited $\text{Cr}_3\text{C}_2\text{-NiCr}$ layer (Fig. 1(a)).

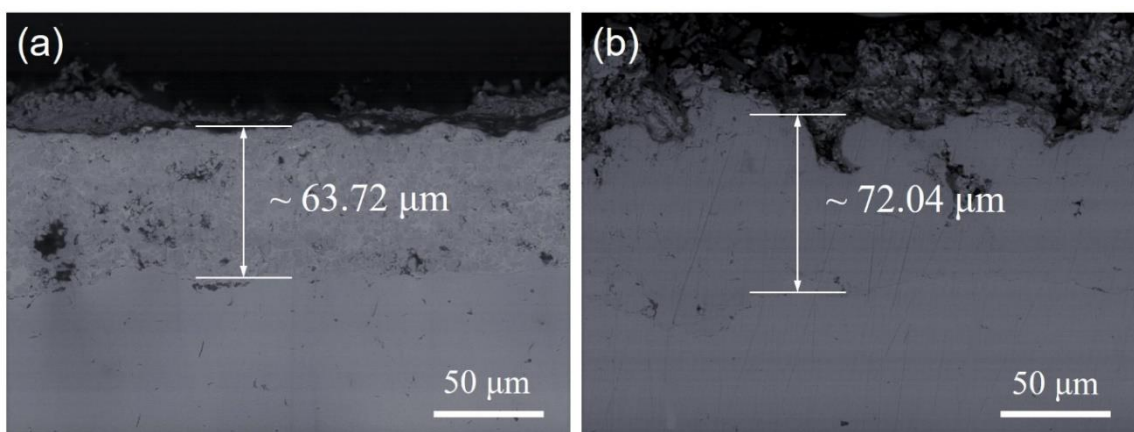


Figure 1. Cross-sectional optical microstructure of Fe-Ni superalloy coated with (a) $\text{Cr}_3\text{C}_2\text{-NiCr}$ and (b) NiCrAlY by HVOF thermal spray coating.

Fig. 2 shows the SEM images of the uncoated Fe-Ni superalloy and the superalloy coated with $\text{Cr}_3\text{C}_2\text{-20%NiCr}$ and NiCrAlY by HVOF thermal spray coating after cyclic hot corrosion in the molten salt environment (75 wt.% Na_2SO_4 + 25 wt.% NaCl) for 5–50 cycles at 900 °C. As shown in the figure, the surface scale of the Fe-Ni superalloy coated with $\text{Cr}_3\text{C}_2\text{-20%NiCr}$ and NiCrAlY was an adherent oxide scale without crack (Figs. 2(a)–(f)). It indicates that the coated materials deposited by HVOF thermal spray coating could be well deposited onto the substrate. Further evaluation on the surface morphologies of the Fe-Ni superalloy coated with $\text{Cr}_3\text{C}_2\text{-20%NiCr}$ (Figs. 2(a)–(c)) and the uncoated superalloy (Figs. 2(g)–(i)) under hot corrosion showed tiny granular structures. Meanwhile, the surface morphologies of Fe-Ni superalloy coated by NiCrAlY layer showed an angular structure (Figs. 2(d)–(f)). This indicates that the presence of Al_2O_3 in the superalloy coated by NiCrAlY can act as a protective oxide, which is beneficial in improving the corrosion resistance. The size of the surface morphology structure increased with increasing cycle number of hot corrosion testing (Figs. 2(a)–(i)).

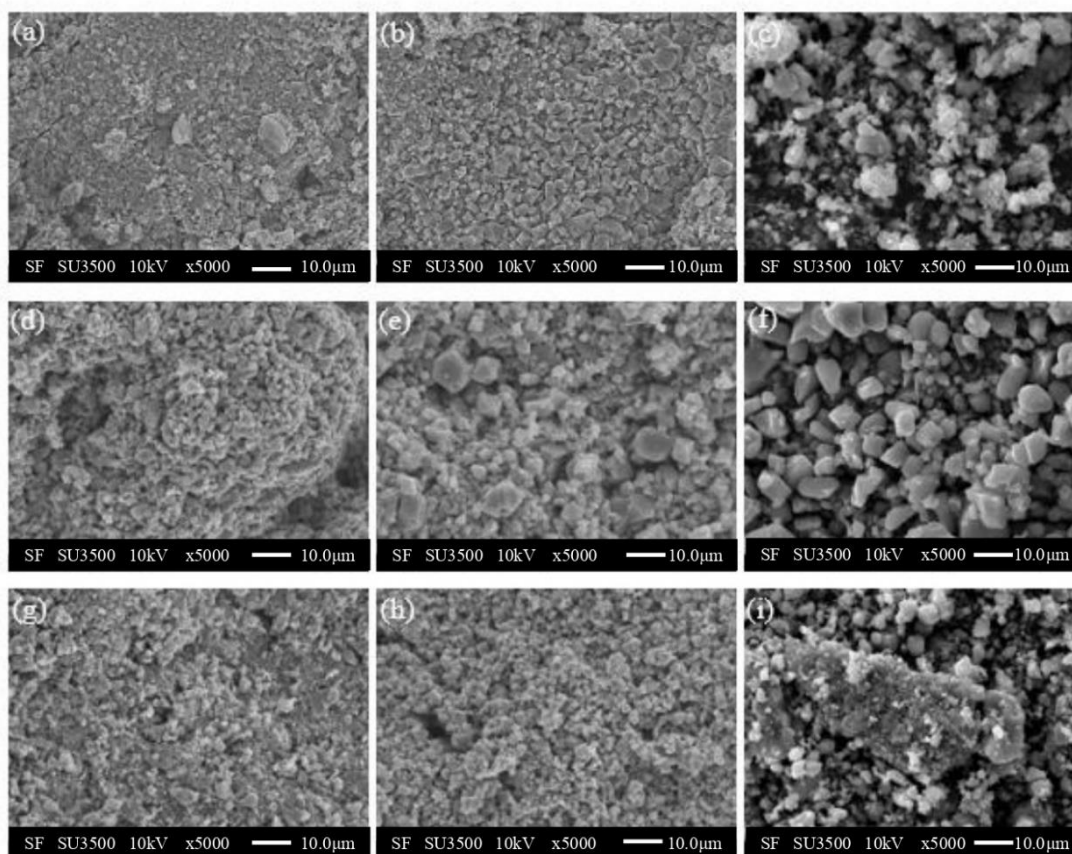


Figure 2. Surface morphologies of the oxide scales formed on the specimen after exposure to molten salt for 5, 25, and 50 cycles. The Fe-Ni superalloy coated with $\text{Cr}_3\text{C}_2\text{-NiCr}$ exposed to (a) 5, (b) 25, and (c) 50 cycles; the Fe-Ni superalloy coated with NiCrAlY exposed to (d) 5, (e) 25, and (f) 50 cycles; the uncoated Fe-Ni superalloy exposed to (g) 5, (h) 25, and (i) 50 cycles.

Fig. 3 shows a cross-sectional image with points of which the elemental composition were measured by using EDS of the uncoated Fe-Ni superalloy and the superalloy coated with $\text{Cr}_3\text{C}_2\text{-20\%NiCr}$ and NiCrAlY layers at some points of near scale, HVOF coating, interfacial layer, and substrate after hot corrosion treatment of 50 cycles ($900\text{ }^\circ\text{C}$) in molten salt environment. The elemental composition quantities of the tested points of EDS shown in Figs. 3(a), (b), and (c) are shown in Figs. 3(d), (e), and (f), respectively. As can be seen, Ni, C, and Fe elements are present in large quantities (point 1). The quantity of Ni and C elements decreased at the tested points, which farther from the uppermost of the surface (Fig. 3(d)). At the tested point of the interfacial region (point 3), the quantity of chemical compositions was relatively similar to that of the substrate of superalloy material (point 4). The cross-sectional SEM images show no cracks in the deposited coating structure. The cross-sectional corroded of Fe-Ni coated with NiCrAlY (Figs. 3(b) and (e)) shows that the oxide scale is mostly homogeneous and that the adherent scale mainly consists of O, Al, and Cr elements, which indicates the formation of Al_2O_3 and Cr_2O_3 . In the subscale region of point 2, the contents of Fe and Ni elements are increased, whereas those of O, Al, and Cr are decreased (Fig. 3(e)). The quantity of O element is decreased at the tested points, which farther from the uppermost of the surface (Figs. 3(d), (e), (f)). Figs.

3(c) and (f) show the cross-sectional image and EDS point analysis of the uncoated Fe-Ni superalloy. As can be seen, the chemical composition mainly consists of Ni and Fe elements. Point 2 shows that the Ni and Fe elements decrease with O and Cr elements are relatively stable (Fig. 3(f)). On the other hand, the quantity of O element decreases up to point 4 (Fig. 3(f)).

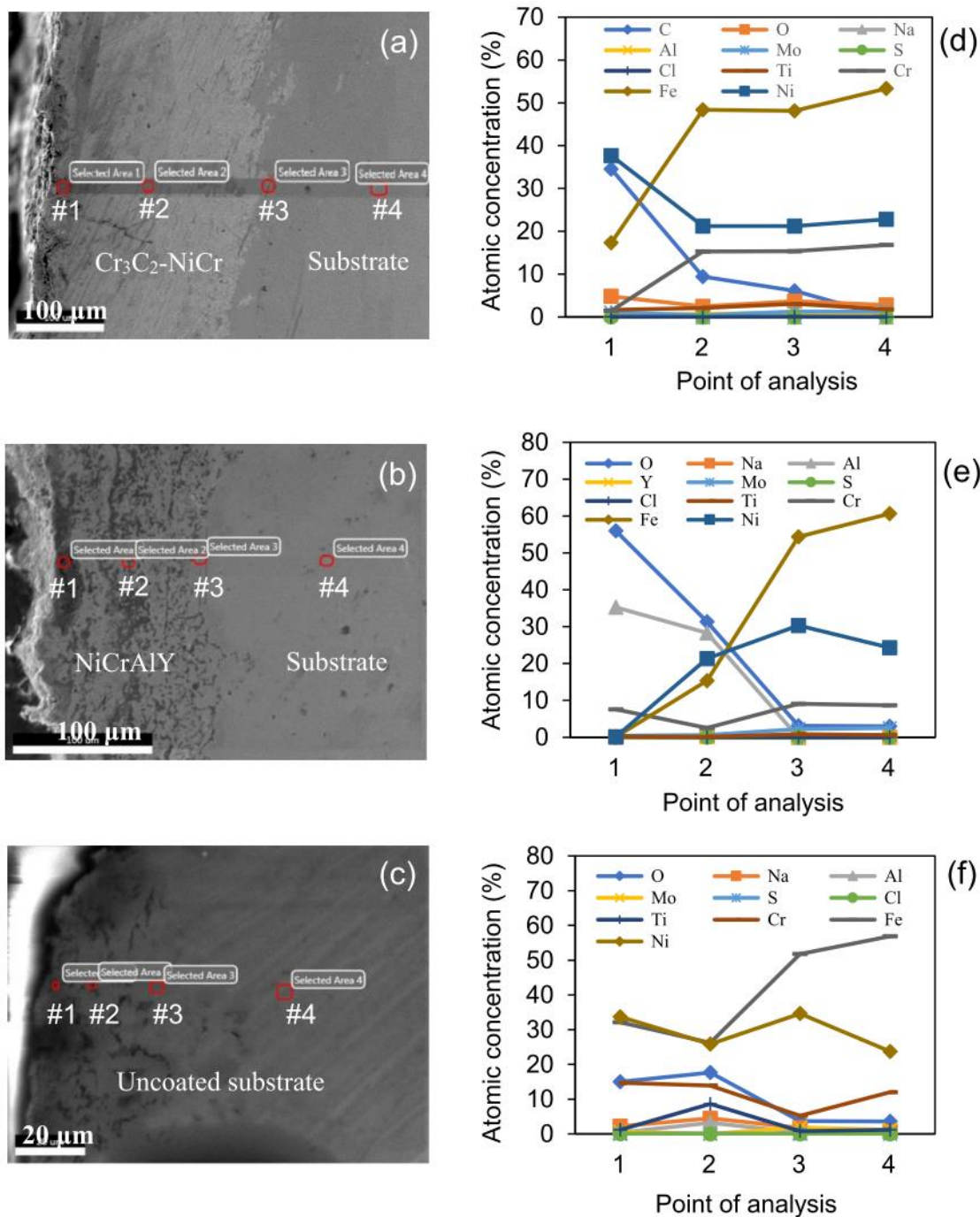


Figure 3. Cross-sectional images and elemental composition of the superalloy coated with $\text{Cr}_3\text{C}_2\text{-NiCr}$ (a, d), superalloy coated with NiCrAlY (b, e), and uncoated Fe-Ni superalloy (c, f) after exposure to the molten salt environment at 900 °C (50 cycles).

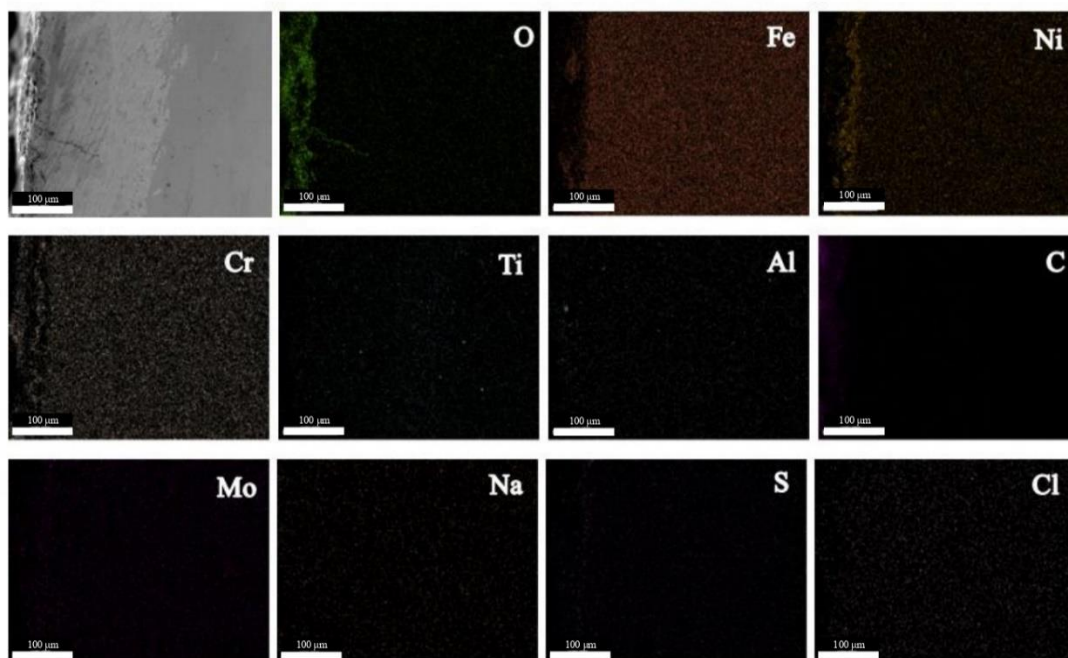
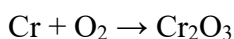


Figure 4. X-ray mapping of cross-sectional Fe-Ni superalloy coated with Cr_3C_2 -NiCr after hot corrosion test in 75 wt.% Na_2SO_4 + 25 wt.% NaCl for 50 cycles (900 °C).

Fig. 4 shows the X-ray mapping of Fe-Ni superalloy coated with Cr_3C_2 -20%NiCr after hot corrosion treatment in 75 wt.% Na_2SO_4 + 25 wt.% NaCl for 50 cycles at 900 °C. As can be seen, the composition mainly consists of O, Fe, Ni, and Cr elements and small amounts of corrosion product such as S, Na, and Cl elements. Matthews et al. [30] reported that Cr might react with O_2 as follows:



Ni reacts with alumina, Fe, and Cr to generate NiCr_2O_4 and NiFe_2O_4 spinels, as shown in the reactions below [31]:



The synthesis of Cr_2O_3 , NiCr_2O_4 , and NiFe_2O_4 spinels in the scale can be linked to the coated Fe-Ni superalloy's hot corrosion resistance. The growth of these oxides along the splat boundaries and within the open pores of the coating may act as a diffusion barrier for corrosive species [27]. The volatile metal chlorides FeCl_2 , NiCl_2 , and CrCl_3 , which are formed when chlorine from NaCl reacts with Fe, Ni, and Cr to generate FeCl_2 , NiCl_2 , and CrCl_3 , may cause cracks in oxide scales [32]. Sulfur from Na_2SO_4 reacts with alloying elements to generate metal sulfides FeS , Cr_2S_3 , and NiS , which can segregate at the oxide scale–substrate interface, causing fast oxidation [33]. This indicates that chlorination and sulfidation mechanisms increase the rate of corrosion.

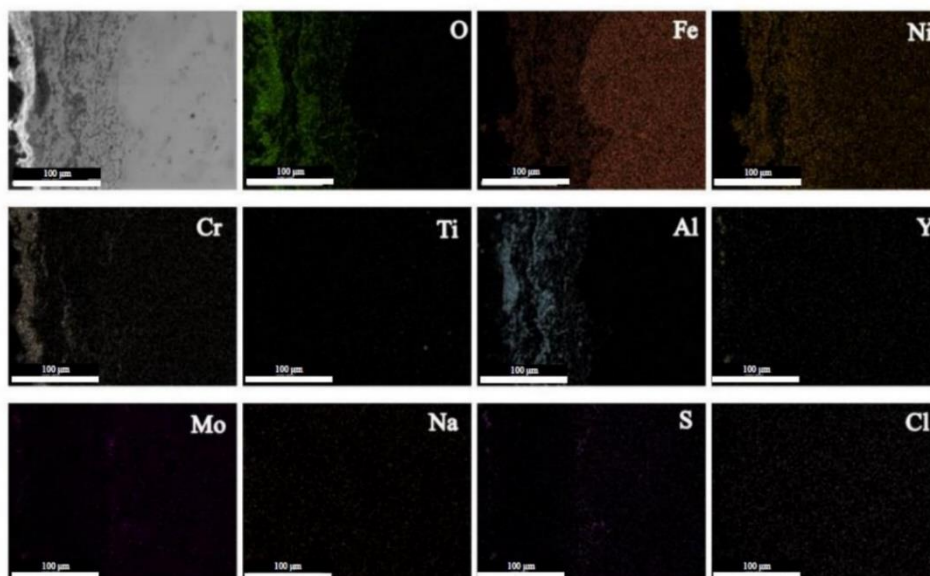


Figure 5. X-ray mapping of cross-sectional Fe-Ni superalloy coated with NiCrAlY after hot corrosion test in 75 wt.% Na₂SO₄ + 25 wt.% NaCl for 50 cycles (900 °C).

Fig. 5 shows the X-ray mapping of cross-sectional Fe-Ni superalloy coated with NiCrAlY after hot corrosion in 75 wt.% Na₂SO₄ + 25 wt.% NaCl for 50 cycles (900 °C). As can be seen, the composition mainly consists of O, Al, and Cr elements and small amount of corrosion products such as S, Na, and Cl elements. Protective oxides such as Al₂O₃ and Cr₂O₃ may partially slow the oxidation of the substrate material by limiting the diffusion of reactive species toward the substrate alloys, as evidenced by the high concentrations of O, Al, and Cr [34]. These oxides are beneficial to the Fe-Ni superalloy by protecting it from the intense corrosive environment.

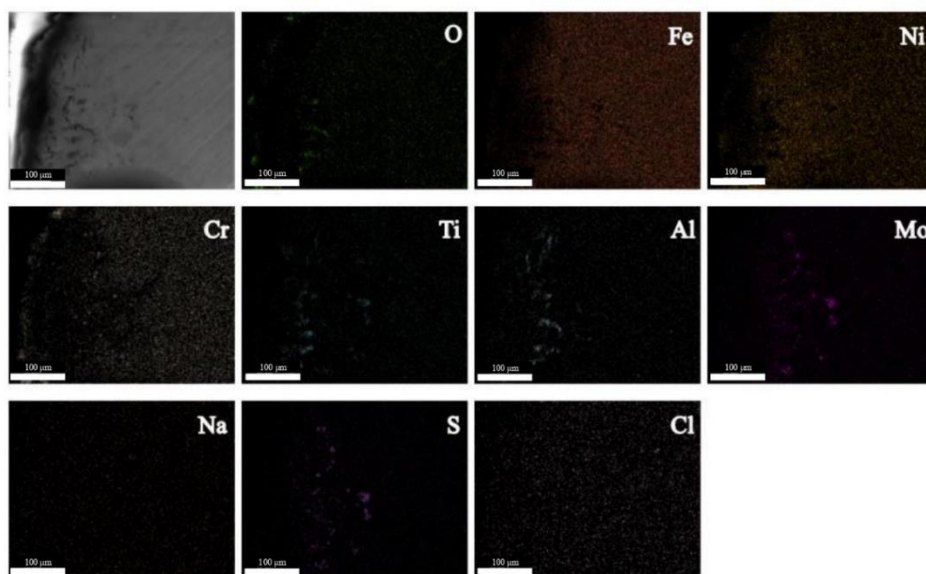


Figure 6. X-ray mapping of cross-sectional uncoated Fe-Ni superalloy after hot corrosion test in 75 wt.% Na₂SO₄ + 25 wt.% NaCl for 50 cycles (900 °C).

Fig. 6 shows the X-ray mapping of uncoated Fe-Ni superalloy after the corrosion test. It mainly consists of Cr, Ti, Al, O, and S elements and small amount of corrosion products. A small amount of Fe was observed in the coating zone, which could be confirmed by the diffusion of Fe from the substrate material (Figs. 3(a), (d) and (b), (e)). The oxide protective layer of Cr_2O_3 does not allow the corrosion products to react with coating alloying elements, resulting in better corrosion resistance.

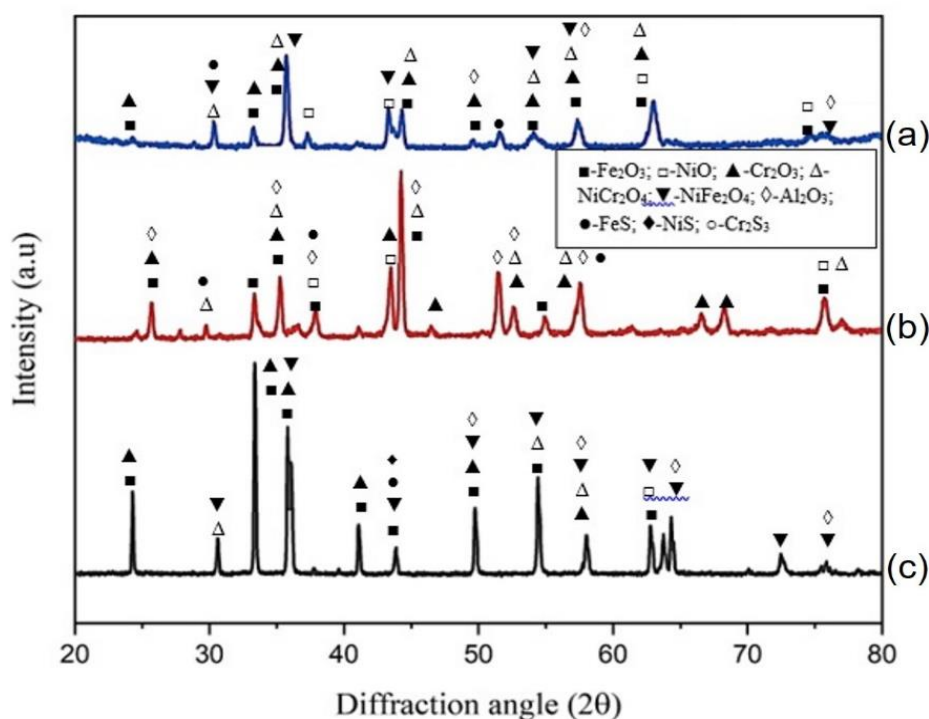


Figure 7. XRD spectra of (a) the uncoated Fe-Ni superalloy, Fe-Ni superalloy coated with NiCrAlY (b), and (c) Cr_3C_2 -20%NiCr after exposure to 75 wt.% Na_2SO_4 + 25 wt.% NaCl for 50 cycles at 900 °C.

Fig. 7 shows the XRD pattern of the uncoated Fe-Ni superalloy and the coated superalloy by HVOF thermal spray coating after hot corrosion test with molten salt of 75 wt.% Na_2SO_4 + 25 wt.% NaCl for 50 cycles at 900 °C. The major phases of the uncoated superalloy are Fe_2O_3 , Al_2O_3 , FeS, and NiCr_2O_4 , with NiFe_2O_4 and NiO as the minor peaks (Fig. 7(a)). On the other hand, the major peaks of the hot corroded Cr_3C_2 -20%NiCr coated specimen are spinel NiCr_2O_4 , Cr_2O_3 , Fe_2O_3 , and Al_2O_3 , with NiO, NiFe_2O_4 , FeS, and NiS as a minor phase (Fig. 7(c)). In the case of Fe-Ni coated with NiCrAlY, Al_2O_3 , Cr_2O_3 , Fe_2O_3 , and spinel NiCr_2O_4 are the major peaks, and NiO and FeS are the minor peaks (Fig. 7(b)). In the XRD spectra of the uncoated Fe-Ni superalloy, NiCr_2O_4 , FeS, Fe_2O_3 , and Al_2O_3 are the major phases. In the oxide scale of corroded Cr_3C_2 -20%NiCr, the spinel NiCr_2O_4 , Cr_2O_3 , Fe_2O_3 , and Al_2O_3 are the major phases. In the Fe-Ni superalloy coated with NiCrAlY, Al_2O_3 , Cr_2O_3 , Fe_2O_3 , and spinel NiCr_2O_4 are the major phases. Fe_2O_3 is the minor phase on the surface of hot corroded Cr_3C_2 -20%NiCr and NiCrAlY, indicating the diffusion of Fe from the substrate during hot corrosion of specimens at 900 °C

[28]. The XRD result shows the presence of metal sulfides such as FeS, CrS, and NiS in the uncoated and coated superalloys as minor phase. This is due to the fact that metal sulfides like NiS, Cr₂S₃, and FeS are created when sulfur from Na₂SO₄ reacts with alloying elements like nickel, chromium, and iron in a reducing environment. Additionally, these sulfides might separate at the point where the oxide scale and substrate meet, which would trigger quick oxidation [27]. At 400 °C, chlorine may dissolve the oxide scales and cause further cracking of the oxide scales. O and Cl permeate through the fissures and react with the substrate alloying components Cr, Ni, and Fe to produce the volatile metal chlorides CrCl₃, NiCl₂, and FeCl₂ [11,27,35]. On the oxide scales, cracks could be caused by the development of volatile chloride. The cracks could then be caused by thermal cycles due to variations in thermal expansion between the substrate material and the oxide scale [36].

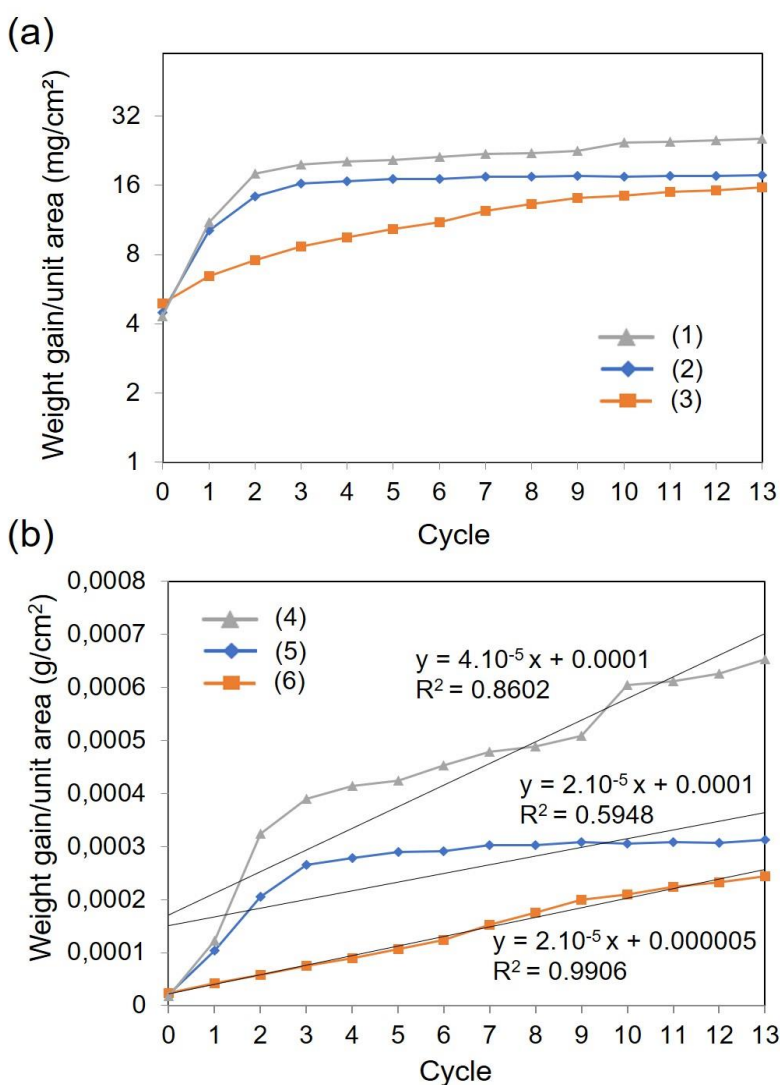


Figure 8. Weight gain after hot corrosion test with molten salt 75 wt.% Na₂SO₄ + 25 wt.% NaCl for 13 cycles. (a) Weight gain measurement of the (1) uncoated Fe-Ni superalloy, (2) superalloy coated with Cr₃C₂-NiCr, and (3) NiCrAlY. (b) Parabolic constant calculated from the data in Fig. 8(a) of (4) the uncoated Fe-Ni superalloy and superalloy coated with (5) Cr₃C₂-NiCr and (6) NiCrAlY obtained by HVOF thermal spray coating.

Fig. 8(a) shows the thermogravimetric analysis (weight gain/unit area) as a function of cycle number of the uncoated Fe-Ni superalloy and the superalloy coated with Cr₃C₂-NiCr and NiCrAlY thermal spray layers by exposing these layers with molten salt of 75 wt.% Na₂SO₄ + 25 wt.% NaCl for 13 cycles. The weight gain of Fe-Ni superalloy coated with NiCrAlY layer is lower than that of Cr₃C₂-20% NiCr layer and the uncoated Fe-Ni superalloy. This indicates that the presence of films provided by HVOF thermal spray coating was able to significantly improve the corrosion resistance of Fe-Ni superalloy in hot environments, with NiCrAlY providing a better corrosion protection than the Cr₃C₂-NiCr layer. In general, the hot corrosion behavior of the uncoated and coated Fe-Ni superalloys follows a nearly parabolic rate law. The parabolic constants (k_p in $10^{-5} \text{ g}^2 \text{ cm}^{-4} \text{ s}^{-1}$) are listed in Table 3. The parabolic constant k_p was calculated by a linear least-squares algorithm to a function in the form of $(\Delta W/A)^2 = k_p t$, where $\Delta W/A$ represents the weight per unit area (g/cm^2) and t indicates the hot corrosion time in seconds (Fig. 8(b)).

Table 3. Parabolic rate constant (k_p)

Sample	k_p ($10^{-5} \text{ g}^2 \text{ cm}^{-4} \text{ s}^{-1}$)
Fe-Ni superalloy coated with Cr ₃ C ₂ -NiCr	7.09
Fe-Ni superalloy coated with NiCrAlY	4.9
Uncoated Fe-Ni superalloy	4.3

As shown in Fig. 8(b), the weight gain curves indicate that all specimens show a relatively high corrosion rate in the first few cycles due to the formation of rapid oxide scale [28, 37]. From the thermogravimetric chart considering the weight loss and the weight gain cycles, the coated superalloys in all cases show much lower weight gain than the uncoated superalloy in the given molten salt. Minor weight gain was observed due to the sputtering of oxide scales outside of the alumina crucible. During the course of hot corrosion experiments, the cumulative weight gain of the uncoated Fe-Ni superalloy, superalloy coated with Cr₃C₂-20%NiCr, and NiCrAlY layers are 25.5678, 17.6659, and 15.6338 mg/cm², respectively, and the parabolic constants (k_p) of the uncoated Fe-Ni superalloy, superalloy coated with Cr₃C₂-20%NiCr, and NiCrAlY layers are 7.09×10^{-5} , 4.9×10^{-5} , and $4.3 \times 10^{-5} \text{ g}^2 \text{ cm}^{-4} \text{ s}^{-1}$, respectively. It clearly indicates that the presence of NiCrAlY and Cr₃C₂-20%NiCr coatings successfully reduces the overall weight gain compared with the uncoated Fe-Ni superalloy (Fig. 8). The NiCrAlY film has the best performance for hot corrosion resistance as indicated by the lowest weight gain.

4. CONCLUSIONS

The HVOF thermal spray coating process was successfully used to deposit Cr₃C₂-20%NiCr and NiCrAlY coating materials onto Ferro Nickel based superalloy (Fe-Ni) substrate. The presence of Cr₃C₂-20%NiCr and NiCrAlY materials on the superalloy significantly improved the corrosion resistance as

indicated by a lower weight gain than the uncoated superalloy. The maximum weight gain of the uncoated superalloy, superalloy coated with Cr₃C₂-20%NiCr, and NiCrAlY is 25.5678, 17.6659, and 15.6338 mg/cm², respectively. The corrosion rates of the uncoated Fe-Ni superalloy, superalloy coated with Cr₃C₂-20%NiCr, and NiCrAlY layers are 7.09×10^{-5} , 4.9×10^{-5} , and 4.3×10^{-5} g² cm⁻⁴ s⁻¹, respectively. The results show that the Fe-Ni superalloy coated with NiCrAlY has better corrosion resistance than the uncoated superalloy and superalloy coated with Cr₃C₂-20%NiCr in NaCl molten salt environment, which can be attributed to its tendency to form a protective dense oxide of Al₂O₃. In the uncoated Fe-Ni superalloy, the corrosive element of sulfur increased the rate of corrosion attack through sulfidation mechanism. In the superalloy coated with Cr₃C₂-20%NiCr, HVOF thermal spray material shows that the corrosive element of chlorine increased the rate of corrosion attack through chlorination mechanism. The mechanism formation of corrosive elements from segregates toward the oxide film-corrosive and diffusion of molten salts.

ACKNOWLEDGMENT

The authors gratefully acknowledge the support of the Department of Metallurgical Engineering of Mining and Petroleum Engineering, Institut Teknologi Bandung (ITB). We thank the technicians of the Research Centre for Advanced Material, National Research and Innovation Agency. We are also grateful for the cooperation and assistance of all research assistants of the Metal Sustainability and Corrosion Laboratory of ITB. This work was supported by National Research and Innovation Agency (Grant No. B-445/V/HK.01.00/2/2022).

References

1. H. De Cicco, M.I. Lупpo, L.M. Griбаudo and J. Ovejero-Garcia, *Mater. Characteriz.*, 52 (2004) 85.
2. J. Alphonsa, V.S. Raja and S. Mukherjee, *Surf. Coat. Technol.*, 280 (2015) 268.
3. B.S. Rho and S.W. Nam, *Mater. Sci. Eng. A.*, 291(2000) 54.
4. S. Chen, M. Zhao and L. Rong, *Mater. Sci. Eng. A.*, 571 (2013) 33.
5. Ó. Martín, P. De Tiedra and M. San-Juan, *Mater. Sci. Eng. A.*, 688 (2017) 309.
6. A.S. Khanna, High Temperature Corrosion, World Scientific Publishing Co. Pte. Ltd., (2016) Singapore.
7. J.S. Hou, J.T. Guo, G.X. Yang, L.Z. Zhou, X.Z. Qin and H.Q. Ye, *Mater. Sci. Eng. A.*, 498 (2008) 349.
8. J.X. Chang, D. Wang, T. Liu, G. Zhang, L.H. Lou and J. Zhang, *Corros. Sci.*, 98 (2015) 585.
9. J.N. Harb and E.E. Smith, *Prog. Energy Combust. Sci.*, 16 (1990) 169.
10. N. Eliaz, G. Shemesh and R.M. Latanision, *Eng. Fail. Analys.*, 9 (2002) 31.
11. A.S. Khanna, High temperature oxidation, In Eds: Handbook of environmental degradation of materials, (2015) William Andrew Publishing, New York, United States of America.
12. D. Deb, S.R. Iyer and V.M. Radhakrishnan, *Mater. Lett.*, 29 (1996) 19.
13. C. Sundaresan, B. Rajasekaran, S. Varalakshmi, K. Santhy, D.S. Rao and G. Sivakumar, *Corros. Sci.*, 189 (2021) 109556.
14. X. Yu, P. Song, X. He, A. Khan, T. Huang, C. Li, Q. Li, K. Lü, K. Chen and J. Lu, *J. Alloys. Compd.*, 790 (2019) 228.
15. W. Brandl, D. Toma and H.J. Grabke, *Surf. Coat. Technol.*, 108 (1998) 10.
16. K. Yamada, Y. Tomono, J. Morimoto, Y. Sasaki and A. Ohmori, *Vacuum*, 65 (2002) 533.

17. N. Bala, H. Singh and S. Prakash, *Mater. Des.*, 31 (2010) 244.
18. B.Q. Wang and Z.R. Shui, *Wear*, 253 (2002) 550.
19. T.S. Sidhu, R.D. Agrawal and S. Prakash, *Surf. Coat. Technol.*, 198 (2005) 441.
20. B.S. Sidhu and S. Prakash, *Surf. Coat. Technol.*, 201 (2006) 1643.
21. T.S. Sidhu, S. Prakash and R.D. Agrawal, *Mater. Sci. Eng. A.*, 430 (2006) 64.
22. G. Marginean and D. Utu, *Appl. Surf. Sci.*, 258 (2012) 8307.
23. R. Edy, P. Budi and H.R. Asyraf, Wear resistance of high velocity oxygen fuel sprayed Cr₃C₂-NiAl-Al₂O₃ coatings, Proceeding of the 1st International Conference on Materials Engineering and AUN/SEED-Net Regional Conference on Materials, Yogyakarta: Universitas Gadjah Mada, Indonesia, (2011) 435-439.
24. W.W. Komang, A.B. Eddy, M. Erie and P. Budi, *J. Biomater. Appl.*, 36 (2021) 375.
25. L. Ajdelsztajn, J.A. Picas, G.E. Kim, F.L. Bastian, J. Schoenung and V. Provenzano, *Mater. Sci. Eng. A.*, 338 (2002), 33.
26. H. Singh, D. Puri and S. Prakash, *Surf. Coat. Technol.*, 192 (2005) 27.
27. S. Kamal, R. Jayaganthan, S. Prakash and S. Kumar, *J. Alloys Compd.*, 463 (2008) 358.
28. H. Wang, X. Yan, H. Zhang, M. Gee, C. Zhao, X. Liu and X. Song, *Ceram. Int.*, 45 (2019) 21293.
29. D. Pradhan, G.S. Mahobia, K. Chattopadhyay and V. Singh, *J. Alloys Compd.*, 740 (2018) 250.
30. S. Matthews, Erosion-corrosion of Cr₃C₂-NiCr high velocity thermal spray coatings, PhD Thesis, University of Auckland, 2004.
31. B. Wang, J. Gong, A.Y. Wang, C. Sun, R.F. Huang and L.S. Wen, *Surf. Coat. Technol.*, 149 (2002) 70.
32. S.M. Jiang, H.Q. Li, J. Ma, C.Z. Xu, J. Gong and C. Sun, *Corros. Sci.*, 52 (2010) 2316.
33. S.M. Muthu and M. Arivarasu, *Eng. Fail. Anal.*, 107 (2020) 104224.
34. A.R. Nicoll and G. Wahl, *Thin Solid Films*, 95 (1982) 21.
35. J. Papp, R.F. Hehemann and A.R. Troiano, Hydrogen embrittlement of high strength FCC alloys, Proceedings of the International Conference on the Effect of Hydrogen on Materials Properties and Selection and Structural Design: Hydrogen in Metals, Pennsylvania: American Society for Metals, United States of America, (1974) 657-669.
36. H.S. Nithin, K.M. Nishchitha, V. Shamanth, K. Hemanth and K.A. Babu, *J. Bio-Tribo-Corros.*, 6 (2020) 28.
37. A.W. Thompson and J.A. Brooks, *Metall. Mater. Trans. A.*, 6 (1975) 1431.